Journal of Alloys and Compounds 505 (2010) 264–267

Contents lists available at ScienceDirect

Journal of Alloys and Compounds

journal homepage: www.elsevier.com/locate/jallcom

Structural and magnetic properties of $Fe_{73.5}Cu_1Nb_{3-x}Ti_xSi_{13.5}B_9$ ($x \leq 3$) alloys

Mi Yan*, Hui Tong, Shan Tao, Junhu Liu

State Key laboratory of Silicon Materials, Department of Materials Science and Engineering, Zhejiang University, Hangzhou 310027, China

ARTICLE INFO

Article history:
Received 10 February 2010
Received in revised form 7 June 2010
Accepted 10 June 2010
Available online 18 June 2010

Keywords:
Finemet alloy
Nanocrystalline grain
Magnetic properties

ABSTRACT

$Fe_{73.5}Cu_1Nb_{3-x}Ti_xSi_{13.5}B_9$ ($x = 0, 1, 2, 3$) amorphous ribbons were prepared by melt spinning technique, then subjected to isothermal treatments for 1 h at 500 and 550 °C, respectively. Differential scanning calorimetry (DSC) measurements show that the α-Fe(Si) phase can be formed over a wider temperature with the increase of Ti content, from 156 °C for $x = 0$ to 164 °C for $x = 3$. Volume fraction of nanocrystalline α-Fe(Si) phase also increases with the increase of Ti content after annealing at 500 and 550 °C for 1 h, which is beneficial to enhance the ferromagnetic exchanging coupling in the alloys. DO_3 ordered superstructure phase formed in the samples with Ti content of 2% and 3%. Better soft magnetic properties were obtained after annealing for 1 h at 550 °C than at 500 °C, accompanied by the enhancement of saturation magnetization from 140.68 emu/g for $x = 0$ to 148.87 emu/g for $x = 3$ and the reduction of coercivity from 3.194 G for $x = 0$ to 1.151 G for $x = 3$.

1. Introduction

Due to the excellent soft magnetic properties [1], $Fe_{73.5}Cu_1Nb_3Si_{13.5}B_9$ alloys (Finemet) have been extensively studied in recent years. Various investigations have been carried out on the preparation process, composition design, crystallization kinetics, microstructure and magnetic properties of $Fe_{73.5}Cu_1Nb_3Si_{13.5}B_9$ alloys [2–4]. Their microstructure is typically composed of nanocrystalline grains embedded in an amorphous matrix after thermal treatment [5]. The excellent soft magnetic properties are related primarily to the exchange coupling between nanocrystalline grains through the amorphous matrix. Generally, Nb is considered as an essential composition element to hinder crystal growth [6], resulting in the formation of nanocrystalline α-Fe(Si) phase with grain size less than the ferromagnetic correlation length ($L_{ex} = 35$ nm) [7]. In order to further improve the soft magnetic properties and to reduce the cost of materials, various researches on the substitution effects of Nb by Mo, V, Mn, Cr and Al have been conducted [8–12]. This work attempts to investigate the substituting effects of Ti for Nb in $Fe_{73.5}Cu_1Nb_{3-x}Ti_xSi_{13.5}B_9$ ($x = 0$, 1, 2, 3) alloys on the crystallization behaviors, microstructure and magnetic properties.

2. Experimental

Master alloy ingots with nominal compositions of $Fe_{73.5}Cu_1Nb_{3-x}Ti_xSi_{13.5}B_9$ ($x = 0, 1, 2, 3$) were prepared by levitation melting the mixture of pure Fe (99.9 wt.%), Cu (99.9 wt.%), Nb (99.5 wt.%), Si (99.99 wt.%) and Fe-B (B 20 wt.%) alloy under the protection of high purity argon. Each ingot was remelted at least three times to ensure its chemical homogeneity. The amorphous ribbons, about 5 mm wide, 20–30 μm thick, were prepared by melt spinning technique. The Cu-wheel surface speed was 40 m/s. In order to obtain the nanocrystalline structure, the ribbons were subjected to isothermal treatments for 1 h at 500 and 550 °C, respectively.

The thermal response of each alloy was analyzed on a Netzsch DSC 404 C differential scanning calorimeter under a continuous argon flow at a heating rate of 10 °C/min, and each sample mass was approximately 1 mg. The phase structure of the ribbons was examined by X-ray diffraction (Rigaku D/max 2550 PC) using Cu Kα ($\lambda = 1.5406$ Å) radiation at an operating voltage of 40 kV. The magnetization hysteresis loops were measured by a Vibrating Sample Magnetometer (Lakeshore 7407).

3. Results and discussion

Fig. 1 illustrates the DSC curves for as-spun $Fe_{73.5}Cu_1Nb_{3-x}Ti_xSi_{13.5}B_9$ ($x = 0$, 1, 2, 3) alloys with a heating rate of 10 °C/min. There are clearly two exothermal main peak positions T_{p1} and T_{p2} on DSC curves for each specimen, corresponding to the enthalpy change and exothermic phase transformations. The first peak at T_{p1} corresponds to the formation of crystalline α-Fe(Si), whereas the second peak at T_{p2} relates to the crystallization of boride Fe_2B [13]. The hard magnetic boride Fe_2B phase is harmful to the soft magnetic properties, so the heat treatment temperature has to be controlled under T_{p2} to avoid the formation of Fe_2B phase [14]. From Fig. 1, it can also be seen that the second shape of peak T_{p2} exhibits a high sharpness pertinent to a strong crystallization process of the boride phase. These results agree well with those reported in Ref. [15].

Table 1 presents the crystallization temperatures T_{p1} and T_{p2} for $Fe_{73.5}Cu_1Nb_{3-x}Ti_xSi_{13.5}B_9$ ($x = 0$, 1, 2, 3) ribbons. The first peak T_{p1} decreases with increasing Ti content, from 533 °C for $x = 0$, to 530 °C for $x = 1$, 522 °C for $x = 2$ and 519 °C for $x = 3$, respectively. The precip-

* Corresponding author. Tel.: +86 571 87952730; fax: +86 571 87952366.
E-mail address: mse_yanmi@zju.edu.cn (M. Yan).

0925-8388/$ – see front matter © 2010 Elsevier B.V. All rights reserved.
doi:10.1016/j.jallcom.2010.06.042

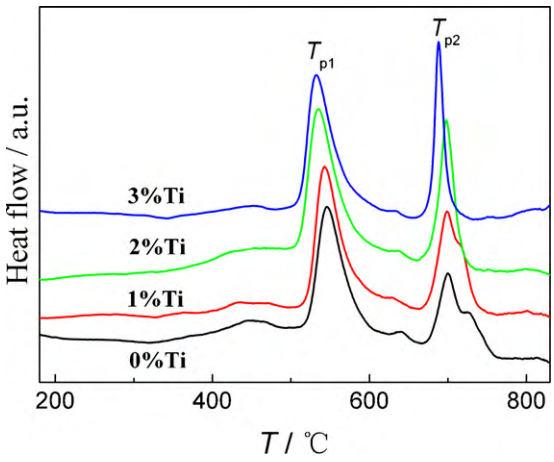

Fig. 1. DSC curves for as-spun $Fe_{73.5}Cu_1Nb_{3-x}Ti_xSi_{13.5}B_9$ (x = 0, 1, 2, 3) ribbons with a heating rate of 10 °C/min.

Table 1
Peak temperatures of crystallization for $Fe_{73.5}Cu_1Nb_{3-x}Ti_xSi_{13.5}B_9$ alloys obtained from the DSC curves in Fig. 1.

x	T_{p1} (°C)	T_{p2} (°C)	$\Delta T_p = T_{p2} - T_{p1}$ (°C)
0	533	689	156
1	530	690	160
2	522	692	170
3	519	683	164

itation temperature of the α-Fe(Si) soft magnetic phase decreases by Ti doping, which means that the α-Fe(Si) phase is easier to precipitate when Ti is present. Meanwhile, the T_{p2} of each sample changes slightly, which is 689 °C for x = 0, 690 °C for x = 1, 692 °C for x = 2 and 683 °C for x = 3, respectively. The range of the peak temperature, $\Delta T_p = T_{p2} - T_{p1}$, increases by doping Ti from 156 °C for x = 0, to 160 °C for x = 1, 170 °C for x = 2 and 164 °C for x = 3, respectively. It indicates that the Ti addition is conducive to the precipitation of α-Fe(Si) phase over a wider temperature region. It can also be inferred that the sample with higher Ti content will precipitate more α-Fe(Si) phase when annealed at the same temperature.

XRD patterns of $Fe_{73.5}Cu_1Nb_{3-x}Ti_xSi_{13.5}B_9$ (x = 0, 1, 2, 3) alloys annealed for 1 h at 500 and 550 °C are shown in Figs. 2 and 3, respectively. When annealed at 500 °C, the diffraction peaks at 2θ = 44.95°, 65.65° and 83.32° for x = 0 can be determined as the (1 1 0), (2 0 0) and (2 1 1) crystalline planes of α-Fe(Si) phase, respectively. It indicates that the annealed samples were partially crystallized after

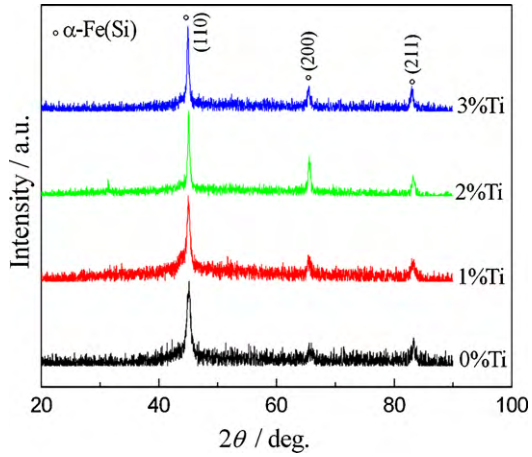

Fig. 2. XRD patterns of $Fe_{73.5}Cu_1Nb_{3-x}Ti_xSi_{13.5}B_9$ (x = 0, 1, 2, 3) alloys annealed at 500 °C for 1 h.

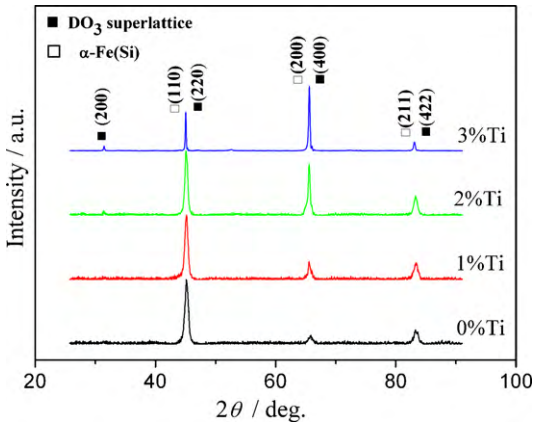

Fig. 3. XRD patterns of $Fe_{73.5}Cu_1Nb_{3-x}Ti_xSi_{13.5}B_9$ (x = 0, 1, 2, 3) alloys annealed at 550 °C for 1 h.

annealing. Crystallized α-Fe(Si) phases are also observed in the other three samples. The diffraction peaks reflect only α-Fe(Si) phase for x = 0 and 1, and new diffraction peaks appears when x increases to 2 and 3 in Figs. 2 and 3. It implies that new crystalline phase precipitates in the samples with higher Ti content. According to previous studies [13,16], the diffraction peak at 2θ = 31.47° can be identified as the (2 0 0) plane of the DO_3 phase, which has an ordered super structure. When annealed at 550 °C, as the Ti content increases to x = 3, the intensity of (2 0 0) peak is enhanced, indicating the increase of the volume fraction of DO_3 phase. The DO_3 phase probably formed when the sample annealed at 500 °C with Ti content of 3%, but the XRD patterns in Fig. 2 does not exhibit the DO_3 phase peaks as there are much more amorphous phase in the samples annealed at 500 °C than annealed at 550 °C, which makes the diffraction peaks of DO_3 phase covered by the noisy patterns of amorphous phase. For samples with the same Ti content, the peaks for α-Fe(Si) phase become more intense and narrower after annealing at 550 °C, which indicates an improvement in the level of crystallinity.

With the increase of Ti content, the peak positions of α-Fe(Si) phase shift to lower Bragg angles. Shifts of peak position in reference to the corresponding position for pure Finemet can be ascribed to the influence of Ti on the basic crystal structures. For the samples annealed at 550 °C, the average lattice parameter of α-Fe(Si) phase calculated from the (1 1 0) peaks, ranges from 0.2833 nm for x = 0, 0.2836 nm for x = 1, 0.2839 nm for x = 2 to 0.2844 nm for x = 3, respectively. The substitution of Ti causes the lattice expansion.

The average grain size of the α-Fe(Si) phase also varies with Ti content. The average sizes of the crystallite phase are estimated from the XRD distributions through Hall–Williamson method (the modified Scherrer formula), in which the effect of strain is also considered [17]:

$$\beta_{\text{sample}} \cos\theta = \frac{K\lambda}{\delta} + 2\varepsilon \sin\theta \quad (1)$$

where β_{sample} is the full width at half-maximum of the Gaussian distribution fitted to the peak, K the Scherrer constant, δ the grain size, λ the wavelength of the X-ray used, ε the internal strain, and θ the Bragg angle. Table 2 lists the average grain size of α-Fe(Si) phase calculated from the X-ray diffraction patterns of each sample after annealing for 1 h at 500 and 550 °C, respectively. The grain size δ increases as Ti content increases, and the largest grain size obtained during this experiment is 23.9 nm, which is still smaller than the magnetic exchange length L_{ex} = 35 nm [7], therefore assuring the soft magnetic properties of Ti doped Finemet alloys. The relative volume fraction of the crystalline phase in each sample can be determined from the areas of the Bragg peaks extracted by

Table 2
Crystalline phase volume fraction calculated from the areas of the Bragg peaks and average grain size of α-Fe(Si) phase calculated from the X-ray diffraction patterns of $Fe_{73.5}Cu_1Nb_{3-x}Ti_xSi_{13.5}B_9$ samples annealed for 1 h at 500 and 550 °C, respectively.

		Ti content x at.%			
		0	1	2	3
Average grain size (nm)	500 °C	9.3	10.2	15.3	21.3
	550 °C	10.6	13.5	16.6	23.9
Volume fraction	500 °C	16.86%	23.82%	34.49%	48.59%
	550 °C	32.09%	39.04%	64.66%	74.20%

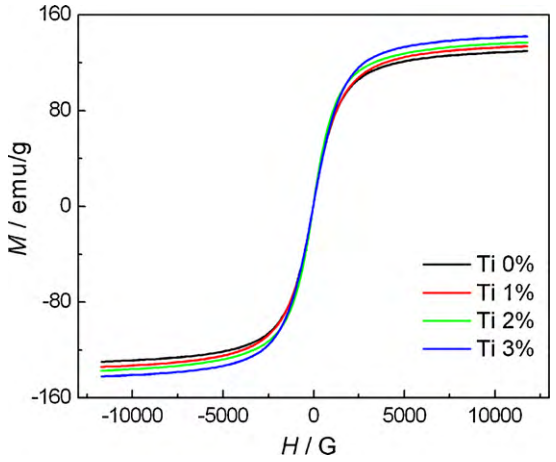

Fig. 4. Magnetization hysteresis loops of $Fe_{73.5}Cu_1Nb_{3-x}Ti_xSi_{13.5}B_9$ (x = 0, 1, 2, 3) alloys annealed at 500 °C for 1 h.

the fit of pseudo-Voigt function [18], which is also summarized in Table 2. The crystalline fraction increases with Ti content, no matter the ribbons were annealed at 500 or 550 °C. According to previous literature [19], a higher level of crystallization will improve the exchange coupling between grains of the soft magnetic phase.

Figs. 4 and 5 show the magnetization hysteresis loops measured in $Fe_{73.5}Cu_1Nb_{3-x}Ti_xSi_{13.5}B_9$ (x = 0, 1, 2, 3) samples after annealing for 1 h at 500 and 550 °C, respectively. All the samples reach a saturated magnetic state in the measured field scope. In comparison with the samples annealed at 500 °C, the samples annealed at 550 °C saturates at much lower fields, showing much weaker magnetocrystalline anisotropy. Based on the law of approach to saturation, saturation magnetization M_S of each sample is calculated. Fig. 6 shows the composition dependences of M_S and coercivity H_C of $Fe_{73.5}Cu_1Nb_{3-x}Ti_xSi_{13.5}B_9$ (x = 0, 1, 2, 3) samples after annealing for 1 h at 500 and 550 °C, respectively. In Fig. 6a, with the increase of Ti content, M_S of the samples annealed at 500 °C increasing from 132.14 emu/g for x = 0, 136.43 emu/g for x = 1, 139.78 emu/g for x = 2 to 144.24 emu/g for x = 3. Meanwhile, M_S of the samples annealed at 550 °C ranges from 140.68 emu/g for x = 0, 140.30 emu/g for x = 1, 141.31 emu/g for x = 2 to 148.87 emu/g for x = 3. It is found that M_S of the samples annealed at 550 °C with Ti content of 0–2% varies slightly, while the sample with 3% Ti has much higher M_S than the others. The volume fraction of nanocrystalline soft magnetic phase of samples with 0, 1 at.% is 32.09% and 39.04%, which means the amorphous phase still plays a dominant role. As a result, the exchange coupling between bcc-Fe nanocrystals of samples with 0, 1% Ti content is nearly the same, which make the M_S varies slightly. The volume fraction of nanocrystalline soft magnetic phase of the sample with 3% Ti is higher than all the other samples. Thus, the intergranular distances will decrease due to the increasing volume fraction of the nanocrystalline phase as well as by the changes in magnetic properties of the retained amorphous matrix, which

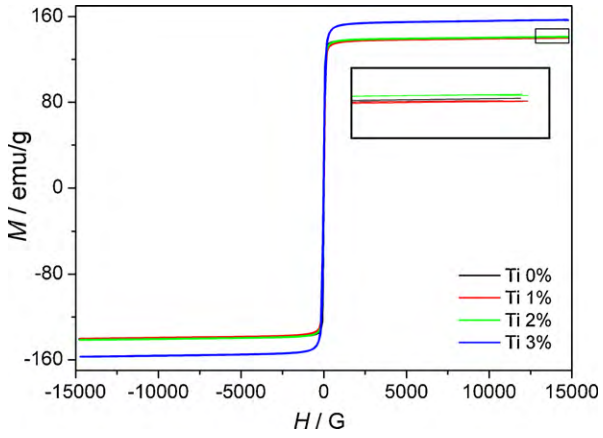

Fig. 5. Magnetization hysteresis loops of $Fe_{73.5}Cu_1Nb_{3-x}Ti_xSi_{13.5}B_9$ (x = 0, 1, 2, 3) alloys annealed at 550 °C for 1 h.

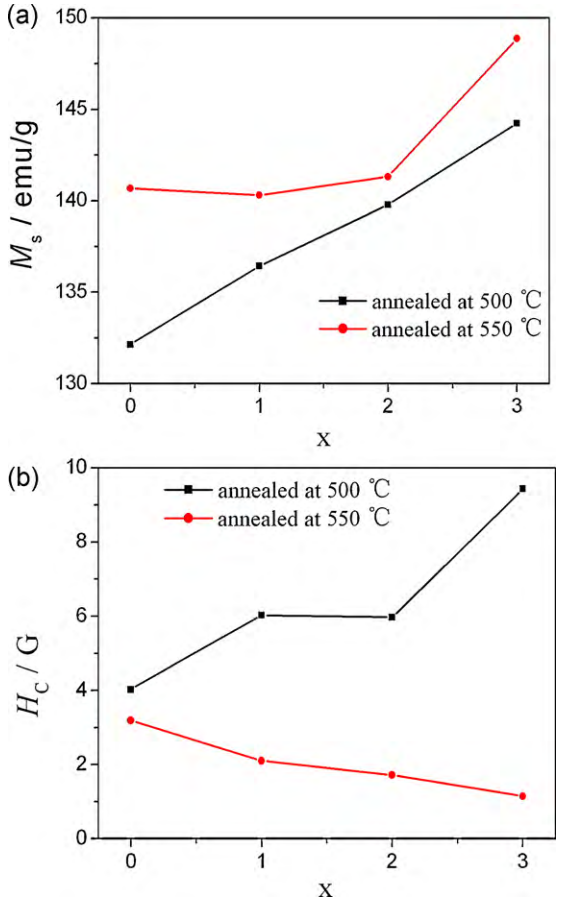

Fig. 6. Composition dependences of (a) saturation magnetization (M_s) and (b) coercivity (H_C) for $Fe_{73.5}Cu_1Nb_{3-x}Ti_xSi_{13.5}B_9$ (x = 0, 1, 2, 3) samples annealed for 1 h at 500 and 550 °C, respectively.

allows stronger exchange coupling between bcc-Fe nanocrystals [20]. For the sample with certain Ti content, M_s of the samples annealed at 550 °C is higher than that at 500 °C because the higher annealing temperature promotes the precipitation of soft magnetic phase. In Fig. 6(b), when annealed at 500 °C, the coercivity of the samples is 4.035 G for $x = 0$, 6.025 G for $x = 1$, 5.971 G for $x = 2$ and 9.429 G for $x = 3$, respectively, which varies irregularly with the increase of Ti content. However, H_C decreases with the increase of Ti content when annealed at 550 °C, with the value of 3.194 G for $x = 0$, 2.101 G for $x = 1$, 1.721 G for $x = 2$ and 1.151 G for $x = 3$. The coercivity of the samples with the same Ti content after annealing for 1 h at 500 °C exhibits higher than that annealed at 550 °C. For samples annealed at 550 °C, the magneto-crystalline anisotropy is randomly averaged out owning to the stronger exchange interaction between nanocrystalline α-Fe(Si) and DO_3 soft magnet phases, as the volume fraction of the nanocrystalline phases increase with the annealing temperature [20]. As a consequence, H_C decreases and therefore the samples exhibit excellent soft magnetic properties. In any case, the samples annealed at 550 °C show better soft magnetic properties than those annealed at 500 °C. In addition, the improvement of the soft magnetic property could also be attributed to the appearance of DO_3 super ordered phase structure. The estimated magnetic moment exerted by one Fe atom in the as-spun sample is about $1.67\mu_B$ on average, while that in a unit cell of the DO_3 phase crystallized from the amorphous is estimated as about $1.85\mu_B$ per Fe atom (about $24.2\mu_B$ per a unit cell of the DO_3 phase) [16]. It demonstrates that Ti is helpful to increase the precipitation of DO_3 ordered structure and therefore improve the magnetic properties.

4. Conclusions

(1) $Fe_{73.5}Cu_1Nb_{3-x}Ti_xSi_{13.5}B_9$ ($x = 0$, 1, 2, 3) amorphous ribbons were prepared by melt-spinning technique. With the increase of Ti content, the formation temperature range of soft magnetic α-Fe(Si) phase is broaden.

(2) When the Ti contents were 0% and 1%, the amorphous samples precipitates only a single α-Fe(Si) phase. When the doping content of Ti exceeds 2%, DO_3 phase appears.

(3) Doping of Ti element improves the level of crystallization of the samples, enhancing ferromagnetic coupling between grains of the magnetic phase. Better soft magnetic properties are obtained in the samples after annealing for 1 h at 550 °C than that annealed at 500 °C.

Acknowledgements

This work was supported by National Natural Science Foundation of China (Grant no. 50971113), Visiting Scholar Foundation of State Key Laboratory of Silicon Materials and the Ministry of Innovative Research Team in University (Grant no. 0651).

References

[1] Y. Yoshizawa, S. Oguma, K. Yamauchi, J. Appl. Phys. 64 (1988) 6044.
[2] M. Stoica, R. Li, A.R. Yavari, G. Vaughan, J. Eckert, N. Van Steenberge, D.R. Romera, J. Alloys Compd. (2010), doi:10.1016/j.jallcom.2010.04.013.
[3] A. Kolano-Burian, R. Kolano, L.K. Varga, J. Alloys Compd. 483 (2009) 560.
[4] H.A. Shivaee, H.R.M. Hosseini, E.M. Lotfabad, S. Roostaie, J. Alloys Compd. 491 (2010) 487.
[5] G. Herzer, IEEE Trans. Magn. 26 (1990) 1397.
[6] J.D. Ayers, V.G. Harris, J.A. Sprague, W.T. Elam, Appl. Phys. Lett. 64 (1994) 974.
[7] G. Herzer, Mater. Sci. Eng. A 133 (1991) 1.
[8] G. Badura, J. Rasek, P. Kwapulinski, Z. Stoklosa, L. Pajak, Phys. Status. Solidi 203 (2006) 349.
[9] B.Q. Chen, S. Yang, X.X. Liu, B. Yan, W. Lu, J. Alloys Compd. 448 (2008) 234.
[10] H.S. Liu, Y. Wu, G.Y. Zhang, C.H. Yin, Y.W. Du, J. Magn. Magn. Mater. 320 (2008) 1705.
[11] K. Brzozka, T. Szumiata, M. Gawrotnski, B. Gorka, P. Sovkak, G. Pavlik, V. Kolesar, Acta Phys. Pol. A 113 (2008) 51.
[12] A. Puszkarz, M. Wasiak, A. Różański, P. Sovak, M. Moneta, J. Alloys Compd. 491 (2010) 495.
[13] R. Brzozowski, M. Wasiak, H. Piekarski, P. Sovak, P. Uznanski, M.E. Moneta, J. Alloys Compd. 470 (2009) 5.
[14] N. Chau, N. Chien, N.Q. Hoa, P.Q. Niem, N.H. Luong, N.D. Tho, V.V. Hiep, J. Magn. Magn. Mater. 282 (2004) 174.
[15] C. Gomez-Polo, J.I. Perez-Landazabal, V. Recarte, IEEE Trans. Magn. 39 (2003) 3019.
[16] H. Okumura, D.E. Laughlin, M.E. McHenry, J. Magn. Magn. Mater. 267 (2003) 347.
[17] G.K. Williamson, W.H. Hall, Acta Metall. 1 (1953) 22.
[18] F. Sánchez-Bajo, F.L. Cumbrera, Appl. Cryst. 30 (1997) 427.
[19] C. GomezPolo, D. Holzer, M. Multigner, E. Navarro, P. Agudo, A. Hernando, M. Vazquez, H. Sassik, R. Grossinger, Phys. Rev. B 53 (1996) 3392.
[20] Z. Wang, K.Y. He, L. Zhang, Acta Metal. Sin. 33 (1997) 1289.